INVITED ARTICLE

PCCP
www.rsc.org/pccp

Self-assembled monolayers of alkanethiols on Au(111): surface structures, defects and dynamics

C. Vericat, M. E. Vela and R. C. Salvarezza*

Instituto de Investigaciones Fisicoquímicas Teóricas y Aplicadas (INIFTA), Universidad Nacional de La Plata - CONICET, Sucursal 4 Casilla de Correo 16 (1900), La Plata, Argentina

Received 29th April 2005, Accepted 22nd July 2005
First published as an Advance Article on the web 9th August 2005

The surface structures, defects and dynamics of self-assembled monolayers (SAMs) on Au(111) are reviewed. In the case of the well-known c(4 × 2) and $\sqrt{3} \times \sqrt{3}$ R30° surface structures, the present discussion is centered on the determination of the adsorption sites. A more complex scenario emerges for the striped phases, where a variety of surface structures that depends on surface coverage are described. Recently reported surface structures at non-saturation coverage show the richness of the self-assembly process. The study of surface dynamics sheds light on the relative stability of some of these surface structures. Typical defects at the alkanethiol monolayer are shown and discussed in relation to SAMs applications.

DOI: 10.1039/b505903h

1. A brief introduction to SAMs

1.1. General aspects of SAMs

The interest that has arisen since the second half of the 20th century in the preparation and characterization of ordered organic thin films (especially monolayers) on well-defined solid surfaces is, apart from the interest in basic knowledge itself, due to their multiple applications in fields like bio-related technology, microanalysis, nano- and microfabrication, in the field of nanodevices, and in corrosion protection, among others.[1–3]

The spontaneous formation of organic monolayers on solid surfaces was first demonstrated in 1946 by Bigelow *et al.* for the case of alkylamines on Pt.[4] Self-assembled monolayers (SAMs) spontaneously form from solution or from vapour phase and combine the advantages of UHV and of the Langmuir–Blodgett method.[5,6] As in the case of UHV-formed films, the method is simple and there is a strong interaction between adsorbate and substrate, since molecules are chemisorbed. On the other hand, as in Langmuir–Blodgett films, chain–chain interactions (involving van der Waals and hydrophobic forces) ensure an efficient packing of the monolayer, and its stability is increased with increasing chain length.[7] In general SAMs with different terminal groups can be easily prepared, and this opens many perspectives regarding their applications. Moreover, SAMs can be formed on objects of all sizes and with a variety of shapes, and not only on planar surfaces.[8,9]

After Bigelow *et al.*'s pioneering investigations, most of the activity in the field of SAMs was initiated in the 80's: in 1980 SAMs of alkyltrichlorosilane on glass, in 1983 SAMs of dialkyldisulfides on Au, and in 1985 SAMs of alkanoic acids on Al_2O_3 were prepared, respectively.[10–12] Nowadays, the most important (and most studied) SAMs are those of alkanethiols ($CH_3CH_{n-1}SH$), and other sulfur head compounds, like disulfides and sulfides, on metals (especially Au, but also Ag, Cu, and even Pt, Fe, and Ni) and semiconductors (GaAs).[5,13] Alkanethiol SAMs, however, do not self-assemble well on hydroxilated surfaces. In that case the most common SAMs are those of silanes (alkyltrichlorosilanes, alkylalcoxysilanes, alkylaminosilanes), which assemble well on SiO_2/Si, Al_2O_3/Al, mica, glass, *etc.*[5a] Other systems of interest are fatty acids on metal oxides (Al_2O_3, AgO, *etc.*), and hydrocarbons on Si.[5a]

1.2. SAMs in nanoscience and nanotechnology

SAMs can be regarded themselves as nanostructures. In fact, they can be regarded as the most elementary form of organic ultrathin film materials. The study of SAMs is particularly promising in the field of sensors, in corrosion prevention, in nanofabrication (especially for information technology), for the construction of nanodevices, for medical implants, and in pharmacology, among others.[1–3,14,15] In many of these applications SAMs can be regarded as the interface between materials with totally different physical and chemical properties: metals, semiconductors, or other inorganic materials, on one hand, and organic and biological materials (polymers, biomolecules, other simpler organic molecules, *etc.*), on the other hand. Also, SAMs have proven to be very useful to stabilize and functionalize nanometre-scale objects like nanoparticles, nanorods and nanowires, *etc.*[2,16,17] Several reviews have been published which deal with different aspects of SAMs on metallic surfaces, especially for planar surfaces, but also for curved surfaces and for nanoparticles. In these reviews the structures, adsorption/desorption kinetics, charge transfer properties, *etc.*, and also the applications of SAMs have been extensively described.[2,5b,13,18–20]

1.3. Experimental methods for SAM studies

SAMs have been studied by many different and complementary surface science techniques, both *ex situ* and *in situ*, like UHV techniques (XPS, AES, LEAD, TPD, GIXD, *etc.*), spectroscopies (IR, Raman, *etc.*), and scanning probe microscopies (STM, AFM, *etc.*) (Table 1).[13a,18,21] The combination of average surface analysis techniques described in Table 1 with the local information from STM/AFM imaging provides a thorough description of the SAMs structures. However, due to the great amount of works that have been published on this field, many performed under very different experimental conditions, some results are contradictory.

As regards STM (scanning tunneling microscopy), this technique was invented at the beginning of the '80s by Binnig, Rohrer and coworkers,[22] and soon started its development, approximately at the same time as SAMs became popular and started to be increasingly studied. Molecular resolution can be

Table 1 Surface science techniques used to study alkanethiolate SAMs on Au(111) that are mentioned in the text

Technique	Main information it provides about SAMs	Ref.
AES	Elemental composition and chemical state SAM coverage	18
AFM	2D SAM structure (also for non-periodic features)	31,53,59,82
GIXD/XRD	2D SAM structures (periodic) Adsorbate–substrate distances	13*a*,30,37,44,50,53
IR spectroscopy	Molecular orientation SAM crystallinity SAM vibrational properties/functional groups	45,77
LEAD	2D SAM structures (periodic)	38
LEED	2D SAM structures (periodic)	30,62
Raman spectroscopy	Molecular orientation SAM vibrational properties/functional groups	18
SFG	Molecular orientation SAM crystallinity SAM vibrational properties	49
STM	2D SAM structures (also for non-periodic features) SAM defects Electronic structure	13*a*,18,19,30,35,40,44,46–49,52,57,58,64,65,67,68,82–86
TPD	Composition SAM adsorption/desorption energies	13*a*
XPS	Elemental composition and chemical state SAM coverage SAM thickness	13*a*,62,63
XSW	Adsorbate-substrate distances	43,51

routinely achieved with STM (and sometimes with contact mode AFM) under a variety of conditions. In contrast to diffraction techniques, STM allow to image non periodic structures like defects of the substrate (vacancies, steps, dislocations, kinks, *etc*.) and of the adsorbate layer (molecular vacancies, missing rows, *etc*.) Further information on this technique can be found in several books.[23–26]

Today, 20 years after its invention, this technique, together with AFM, has proven to be an essential tool to investigate surface structures at the molecular level. Most of the direct structural and local information on SAMs arises from STM imaging. Despite the fact that STM images result from a convolution between topographic and electronic effects that requires careful interpretation, its higher spatial resolution compared to AFM has made this technique the most popular to explore SAMs at the molecular level. In fact, STM images usually exhibit a larger richness of features than AFM images.

2. Alkanethiols on Au(111)

2.1. General aspects

Alkanethiol SAMs on metals, and particularly on Au, have attracted considerable attention due to its ease of preparation and to the strength of the S–Au bond. These monolayers are very stable once prepared, and they are not sensitive to moisture, and do not polymerize, in contrast to SAMs of silanes, which hydrolize and form polymers that can contaminate the surface. Alkanethiol SAMs on Au are also unique as regards the diversity of applications, among which are (i) the modification of the wetting properties of surfaces and lubrication, (ii) the development of new methods of pharmacological dosage, (iii) the immobilization of different species or functional groups for sensors and biosensors, (iv) the development of nanodevices for electronics and of new methods of nanofabrication, (v) their use as templates for crystallization of inorganic salts.[1–3,14,15,27–29]

A thiol molecule consists of three parts: the sulfur head, the hydrocarbon chain (of variable length), and the terminal group, which can have different functionalities (Fig. 1). The energy related to each part of the molecule has a different order of magnitude: 50 kcal mol^{-1} for the interaction between the S head and the substrate (a thiolate bond); 1–2 kcal mol^{-1} per methylene for the van der Waals interactions between hydrocarbon chains; and only a few kT for energies related to the terminal groups.[5*b*] However, all three parts of the molecule contribute to the structure and to the physical and chemical properties of the SAMs.

Alkanethiolate self assembly on gold is easy to perform and can be done both in gas-phase and in liquid environments (from solutions of different solvents), the latter being by far the most popular method because of its simplicity and accessibility in most laboratories. In general, alkanethiol adsorption on gold is performed in 10–1000 μM solutions of thiols or disulfides (in the latter case the S–S bond breaks upon adsorption) in different solvents depending on the nature of the thiol, and for different adsorption times (2–12 h for long chain thiols; at least 24 h for short chain thiols).[18]

Several factors affect the quality of the thiolate SAMs. In the case of SAMs formed in solution we can mention the

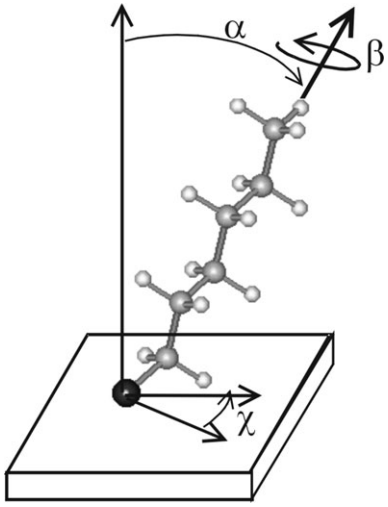

Fig. 1 Scheme of an alkanethiolate molecule adsorbed on Au(111) in a standing up configuration (stable phase). The angles are $\alpha = 30°$, $\beta = 55°$, and $\chi = 14°$. Black circle: sulfur atom, gray: carbon atoms, white: hydrogen atoms.

crystallinity and the roughness of the gold substrate (as well as its cleanliness), the nature of the adsorbate (the hydrocarbon chain length, the terminal group functionality, *etc.*), the temperature at which the thiol is adsorbed, the solvent used (ethanol, methanol, toluene, hexane, water, *etc.*), the immersion time, and the concentration of adsorbate, among others.[2,18] Because of the above mentioned factors, the idea of a "perfect" self-assembled monolayer is far from reality, due to the existence of different types of defects, as it will be discussed below.

Until recently, SAM formation was thought to proceed *via* simple Langmuir-type kinetics. However, the recent discovery of the existence of lower density phases (the so called "striped" phases) and measurements of the rate of thiol adsorption on gold surfaces by STM, XRD and LEED and atomic beam scattering have indicated that SAM growth from the vapor occurs in at least two steps.[30] Recent AFM studies suggest that this is also true for SAM growth from butanolic solutions.[31] Furthermore, during gas phase deposition, the growth rate shows a complex dependence on pressure with three regimes: linear, quadratic, and saturated growth.[13a] The simplest picture of this process implies an initial physisorption, followed by chemisorption of the molecules on the Au through the S-heads (a process that takes minutes), and finally the slow formation of ordered domains (a process that can take several hours, or even days).[30–33] The ability of alkanethiols to both physisorb through van der Waals interactions and to chemisorb through the sulfur head provides an opportunity to study the role of the physisorbed precursor state in the chemisorption kinetics. Conversely to that observed for physisorbed alkanethiols on HOPG,[34] the physisorbed state on Au(111) can be described as a gas-like, highly disordered system.

Upon physisorption, the alkanethiol molecule binds to the Au(111) substrate through the S head and then it loses the mercaptan H atom, transforming itself in an alkanethiolate. Ordered flat-lying surface structures known as striped phases are then formed. The increase in the surface coverage results in the nucleation of standing-up domains that finally cover the entire Au(111) surface. The molecules on the substrate surface can then be described by three angles: the molecular tilt (α), the angle of rotation of the hydrocarbon chain plane about the molecular axis (β), and the angle of precession (χ), which defines the tilt direction and is derived from the projection of the inclination plane (defined by the substrate normal and the axe of the hydrocarbon chain) on the substrate plane.[13a,35] This is schematically shown in Fig. 1.

Due to the strong interaction between the alkanethiol molecule and the Au(111) substrate, the S head chemisorbs on specific sites of the substrate, thus forming commensurate lattices on the Au (1 × 1) lattice. Stable lattices at saturation coverage are the $\sqrt{3} \times \sqrt{3}$ R30°[36] and its related c(4 × 2) superlattices,[37,38] although others such as the striped phases can be found in the case of non-saturated coverage.

Still today, our knowledge of alkanethiolate SAMs on Au(111) is at least incomplete. Even in the case of the well known c(4 × 2) and $\sqrt{3} \times \sqrt{3}$ R30° surface structures there is controversy about the actual adsorption site(s) involved. This subject is not only an academic problem, but also an important issue with practical implications. In fact, this knowledge is relevant for molecular electronics, and also for electron transfer from/to redox species and biomolecules immobilized on SAMs that can be used in sensors and biosensors. Also, it has been shown that the conductance of a single-thiol molecule changes with the adsorption site.[39]

On the other hand, a family of lattices of lower coverage has been observed. Some confusion exists in the literature, particularly concerning the so-called striped phases, so that new efforts are needed to determine the surface structure and possible adsorption sites involved in those lattices. Other crucial problems are SAM defects and surface structure dynamics, both items having strong implications for possible technological uses of SAMs. A review of these important issues (surface structures, defects and dynamics), based on evidence from STM (and AFM) measurements, is the aim of this work.

2.2. The $\sqrt{3} \times \sqrt{3}$ R30° alkanethiolate lattice on Au(111)

In the $\sqrt{3} \times \sqrt{3}$ R30° alkanethiolate lattice all surface sites are equivalents. This lattice presents distances of 0.499 nm between the S heads of nearest neighbour molecules. The unit cell contains one molecule and its area is 0.2165 nm^2. The surface coverage θ is 0.33 and the tilt angle $\alpha = 30°$. In Fig. 2a a top view STM image of this lattice is shown. The bright spots indicate the position of the alkanethiolate species. As STM senses the electronic density at the Fermi level, it is not completely clear if the spots correspond to the S head or to the alkyl chains of the chemisorbed molecules.[18,40] As mentioned before, even for this simple lattice (with all equivalent sites), the specific adsorption site (Fig. 3) of the alkanethiolate molecule on the Au(111) lattice has not been unambiguously assigned. In fact, density functional theory (DFT) calculations of the most favourable adsorption sites for methanethiolate (CH_3S) on Au(111) performed by different research groups yield completely different results. Hexagonal closed-packed and face-centered cubic, hollow, bridge, and their intermediate (fcc-bridge and hcp-bridge) sites have all been regarded as the preferred sites for alkanethiolate adsorption on the Au(111) face.[41] The reasons of this discrepancy could be limitations of the calculation methods, or the presence of local energy minima.

The general picture of the $\sqrt{3} \times \sqrt{3}$ R30° alkanethiolate lattice that we had until some time ago was that the S heads were placed in equivalent sites somewhere between the fcc hollow and the bridge site (Fig. 3). Recently, however, an unexpected experimental result has been reported by two different groups employing different experimental techniques. In fact, it has been found from XPD[42] and from normal incidence XSW[43] studies of $\sqrt{3} \times \sqrt{3}$ R30° methanethiolate lattices on Au(111) formed from the gas phase that alkanethiolate adsorption would take place at on-top sites. It should be noted that all DFT calculations agree on the fact that the adsorption energy of alkanethiolate molecules at top sites is the smallest (less favorable) among the usually considered Au(111) sites.[41]

Very recently, GIXD results for dodecanethiolate SAMs on Au(111) have revealed the existence of incoherent domains of

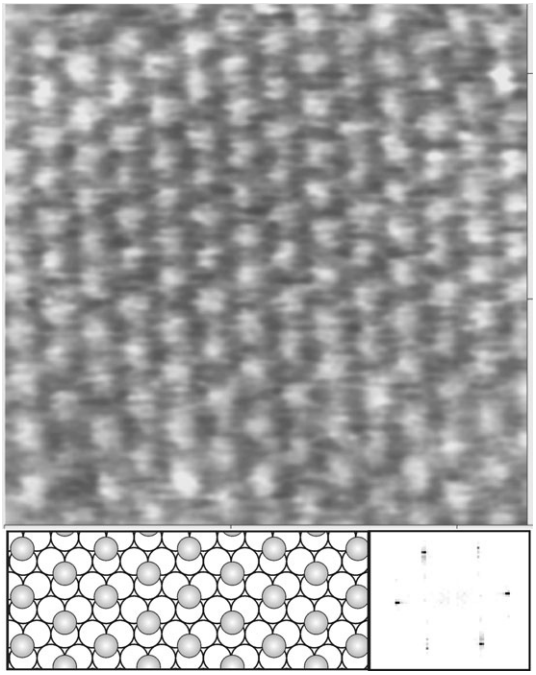

Fig. 2 5.77 × 5.77 nm^2 STM image of the $\sqrt{3} \times \sqrt{3}$ R30° hexanethiolate domain on Au(111). E_{bias} = 465 mV, i_t = 739 pA. Bottom left: scheme showing the $\sqrt{3} \times \sqrt{3}$ R30° lattice. The selection of the Au binding sites (in this case hollow sites) is arbitrary (see discussion) Gray circles: alkanethiolate molecules, white circles: gold atoms. Bottom right: Fourier transformation corresponding to the hexagonal pattern.

alkanethiolate molecules at on-top and fcc hollow sites.[44] A two-adsorption site model for dodecanethiolate $\sqrt{3} \times \sqrt{3}$ R30° lattices on Au(111) has been proposed that reconciles DFT calculations with the experimental data by introducing kinetical considerations. The presence of dodecanethiolate molecules at these two sites could be explained by a two-step adsorption kinetics. In fact, DFT calculations have shown that alkanethiol physisorption involves on-top sites due to steric reasons.[41b] Once the molecule becomes chemisorbed (by losing the mercaptan H), it can eventually diffuse from the top site to the energetically more favourable fcc sites. This last step depends on the energy barrier arising from the van der Waals interactions between adjacent molecules, and could be the reason for finding domains of "frozen" molecules at on-top sites in addition to domains of molecules at the more stable fcc hollow configuration, as shown schematically in Fig. 2. The idea that some domains of alkanethiolate molecules can be trapped at local minima by weak forces is attractive because it could explain some aspects of the complex dynamics observed in alkanethiolate lattices, and thus it should be further investigated.

2.3. The c(4 × 2) superlattice

The very first evidence of the existence of a structure other than the $\sqrt{3} \times \sqrt{3}$ R30° was found from low temperature IR measurements, when the splitting of a vibrational mode of the CH_2 was detected.[45] The existence of other stable and ordered surface structure was later confirmed by LEAD[38] and GIXD[37] experiments: there were diffraction peaks that could not be explained on the basis of a simple hexagonal lattice. These surface structures, which have the same coverage and tilt angle ($\alpha = 30°$) as the $\sqrt{3} \times \sqrt{3}$ R30°, were described as c(4 × 2) superlattices of the $\sqrt{3} \times \sqrt{3}$ R30° lattice, though it is more correct to describe them as (3 × 2$\sqrt{3}$)rect, taking into account the registry with the substrate. The c(4 × 2) superlattice unit cell is orthorombic, and its dimensions are 0.9994 nm × 0.8655 nm (Fig. 4). This unit cell is four times that of the $\sqrt{3} \times \sqrt{3}$ R30° lattice, which means it contains four molecules.

The c(4 × 2) lattice is still a matter of controversy, and several models to explain this structure have been proposed. Since, for sterical reasons, α and χ (Fig. 1) can only have a single value for domains of closely packed alkanethiolate lattices, one of the models proposes that the origin of the c(4 × 2) superlattices would be rows of molecules with two different β values (with a 90° difference), which would result in a different height of the terminal group. Two structures fulfil this requirement and are compatible with LEAD data: a) a hydrocarbon chain with a β value and three chains with a 90°-rotated β; b) two chains with the same β value and two with a 90°-rotated β. The second option was preferred by the authors in ref. 38 because of its higher symmetry.

On the other hand, structures have been found by STM that can be described as c(4 × 2) superlattices and that have unit cells that coincide with that found from diffraction techniques.[35,46–48] There seems to be more than one structure compatible with the unit cell. Among the most common ones are the zig-zag c(4 × 2) (Fig. 4a), with two chains with a β value and other two with a 90° difference, and the rectangular c(4 × 2) (Fig. 4b), with three chains with a β and another one with a 90° difference. These two structures are the same as those proposed from LEAD data.[38]

However, it has been argued from GIXD results that differences in β would not be enough to explain the data, and that there should be a displacement of the S heads with respect

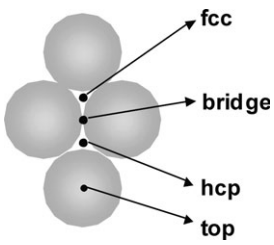

Fig. 3 Possible adsorption sites for an alkanethiolate molecule on the Au(111) unit cell.

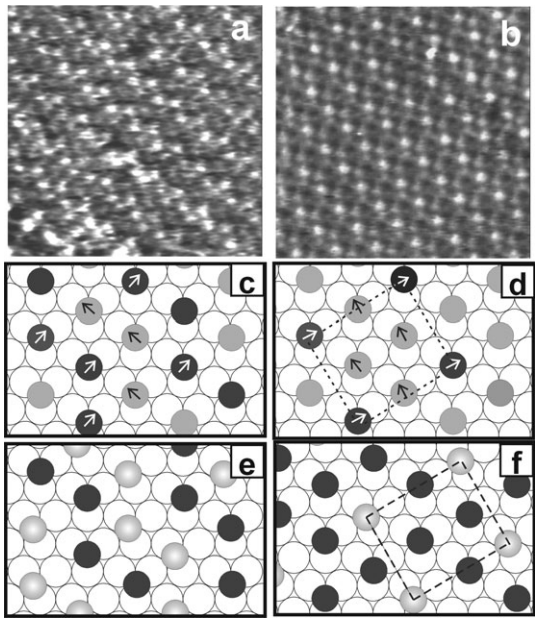

Fig. 4 STM images of hexanethiolate c(4 × 2) lattices: (a) zig-zag (7.3 × 7.3 nm^2) E_{bias} = −965 mV, i_t = 205 pA (b) rectangular (7.3 × 7.3 nm^2). E_{bias} = 800 mV, i_t = 800 pA. Schemes for the c(4 × 2) lattices: (c) zig-zag, (d) rectangular, according the "chain tilt" model (ref. 38). The arrows indicate the projection of the hydrocarbon chain plane (χ angle). (e) zig-zag , (f) rectangular, according to the "two site model" (ref. 52). The unit cells are drawn. Black and gray circles: alkanethiolate molecules, white circles: gold atoms.

to the $\sqrt{3} \times \sqrt{3}$ R30° lattice.[37] The problem is then to determine the magnitude of this displacement. This idea is supported by a SFG study whose main conclusion is that the alkanethiolate S heads should occupy non-equivalent sites of the substrate.[49] Several models can be found in the literature.

A model based on GIXD measurements has been proposed in which adsorbed alkanethiolate molecules would adsorb forming disulfides with 0.22 nm S–S distances.[50] To achieve this, molecules should present gauche defects in the S–C bond, so that the hydrocarbon chains can have a hexagonal closed packing. According to this model, one of the S atoms of the disulfide would be placed in an fcc hollow and the other one in a bridge site. However, although many efforts were made to detect this dimer by different techniques, there has been no clear experimental evidence in support of this model, with the exception of a XSW work where a different dimer was proposed, with only one of the S atoms attached to the gold substrate.[51]

On the other hand, after careful measurements, the analysis of the distances between bright spots in STM images has revealed that the distances between the molecules in the brightest rows and those in the less bright rows are actually of 0.45 nm (and not 0.5 nm). This has inspired another model, in which the molecules of the darker rows are in one type of site (*e.g.*, hollow site), and those in the brighter rows are in another type of site (*e.g.*, bridge).[52] An additional contribution from differences in β could also be possible.

The schemes in Fig. 4c–f show surface structures for the model proposed in ref. 38 and for the model described in ref. 52 for the c(4 × 2) lattices, respectively. Note that these schemes are only to help the reader to understand the STM images shown in Fig. 4. The position of the alkanethiolate molecules on the substrate is highly speculative because, as in the case of the alkanethiolate $\sqrt{3} \times \sqrt{3}$ R30° lattice, it is not clear which are the actual Au sites involved in the chemisorption.

Another model has been recently proposed for the c(4 × 2), also on the basis of GIXD data, in which S atoms are located in adjacent fcc and hcp hollow sites, with no evidence of pairing or dimer formation.[53] There is evidence of substrate reconstruction, and while the lateral and normal relaxations of the Au atoms are small, this effect plays an important role for the c(4 × 2) structure.

Nowadays, the model that proposed the formation of S–S bonds in the c(4 × 2) lattice has been discarded, and although there is agreement on the fact that some pairing of the S heads may exist, the magnitude of the S atoms displacement with respect to the $\sqrt{3} \times \sqrt{3}$ R30° lattice is still matter of discussion. What is evident is that the c(4 × 2) surface structure deserves further investigation.

2.4. The relative amount of $\sqrt{3} \times \sqrt{3}$ R30° and c(4 × 2) lattices

The relative amount of $\sqrt{3} \times \sqrt{3}$ R30° and c(4 × 2) domains at alkanethiolate SAMs is another controversial point because of the variety of adsorption conditions and substrate preparations described in the literature. The general question would be: is there some trend for the $\sqrt{3} \times \sqrt{3}$ R30°/ c(4 × 2) surface concentration ratio, based on hydrocarbon chain length and temperature? GIXD analysis has shown that for long chain alkanethiolate SAMs on Au(111) ($n > 11$) the amount of the c(4 × 2) superlattice is smaller than that of the $\sqrt{3} \times \sqrt{3}$ R30° lattice, while for medium-length alkanethiolate SAMs ($n = 6$) the c(4 × 2) structures are predominant. In fact, for $n = 12$ and 16 at room temperature a negligible amount of c(4 × 2) has been observed by GIXD and STM/AFM.[44,53] The relative amount of the c(4 × 2) lattice increased to 40% only after careful annealing at T = 40–55 °C.[53] Even if it has been reported that the c(4 × 2) is the most stable structure, there are evidences that both lattices have almost the same energy. On the other hand, XPD data have indicated that for short alkanethiolates the $\sqrt{3} \times \sqrt{3}$ R30° lattice is the predominant surface structure,[43] although STM data clearly show that this surface structure exhibits alternating missing rows leading to the so-called "pinstripe" lattices, as discussed below.

2.5. Other surfaces structures

A variety of striped phases for alkanethiolates on Au(111) (Fig. 5) has been reported in the literature, and there is some confusion about the molecular arrangement involved in these lattices. Striped $p \times \sqrt{3}$ phases (p being an integer or half-integer multiple of the Au 0.288 nm distance) have been observed at early stages of growth from the vapour phase both on non-reconstructed (1 × 1) and reconstructed (22 × $\sqrt{3}$) Au (111) surfaces.[32,54,55] In the case of octanethiol and decanethiol, 23 × $\sqrt{3}$ and 11.5 × $\sqrt{3}$ surface structures have been reported.[55] These phases have been assigned to lying down molecules in different arrangements, as shown in Fig. 6.

When molecules adopt S-head to S-head configurations, p is chain dependent and twice of that found for the bulk molecule. Striped phases with 2.3 nm separation are also formed at the early stage of hexanethiolate adsorption on Au(111) from ethanolic solutions.[56] This distance is nearly twice the overall length of the molecule, implying a head to head orientation. When the surface coverage increases, islands of $\sqrt{3} \times \sqrt{3}$ R30° and c(4 × 2) nucleate inside the lying down phases, which finally disappear.[32,54]

Striped-like phases with a completely different molecular structure, also described as $p \times \sqrt{3}$, have been observed both in air and *in situ* in pure alkanethiol liquids. Yamada and Uosaki[33] have published a study of the self-assembly mechanism of alkanethiols on Au(111) in solution. They have observed the $\sqrt{3} \times \sqrt{3}$ R30° structure 30–60 minutes after a decanethiol solution was added to the cell. Two parallel stripe structures of different periodicity were imaged. The wider stripes were attributed to molecules lying flat on the surface, but the narrow stripes were attributed to standing-up molecules.

Similar results were reported by Kobayashi *et al.*[57] In this work STM images of octanethiol monolayers on Au(111) showed that the SAM consisted of the $\sqrt{3} \times \sqrt{3}$ R30° lattice structure, the c(4 × 2) superlattice, and striped structures which had a unit cell of $p \times \sqrt{3}$. In this case it was proposed that these striped structures were made of molecules which were not parallel to the surface, but packed with a larger tilt angle than in the case of common ordered domains.

The real nature of some of these lattices, however, has been clarified by high resolution STM imaging. In Fig. 7a a 6 × $\sqrt{3}$ butanethiol lattice is shown. Between the bright stripes the presence of the hexagonal array corresponding to the $\sqrt{3} \times \sqrt{3}$ R30° with d = 0.5 nm (*i.e.* molecules in a standing-up configuration), is clearly resolved (Fig. 7a, inset). In this case the

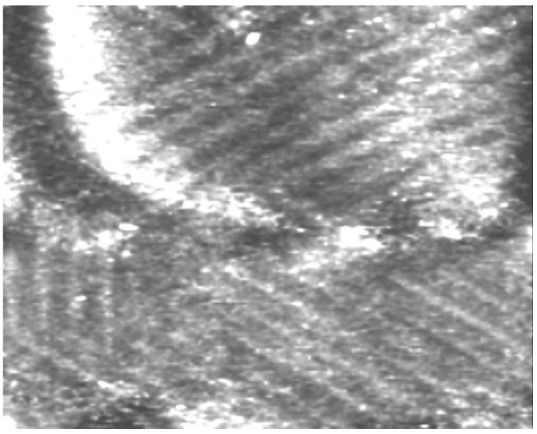

Fig. 5 24.3 × 19.3 nm^2 STM image showing different striped phase domains for propanethiolate on Au(111). E_{bias} = 200 mV, i_t = 794 pA.

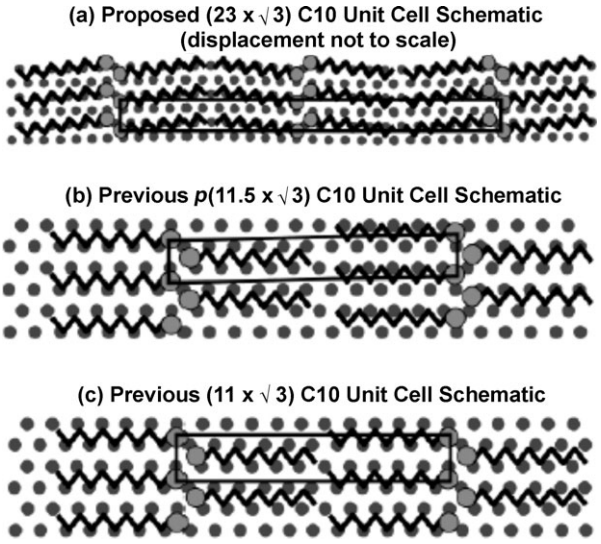

Fig. 6 (a) 23 × $\sqrt{3}$ unit cell (C10), (b) 11.5 × $\sqrt{3}$ unit cell (C10), (c) 11 × $\sqrt{3}$ unit cell (C10). Reprinted with permission from ref. 55 (Copyright 2005 American Chemical Society).

different contrast of the rows that leads to the $p \times \sqrt{3}$ superstructure has been assigned to alkanethiolate molecules placed in different sites (hcp and fcc).[52] Real time imaging has shown that these lattices are metastable and slowly transform into the $\sqrt{3} \times \sqrt{3}$ R30° lattice.[52] A scheme for this lattice is shown in Fig. 7b.

This type of $p \times \sqrt{3}$ phases are also dominant in SAMs of 3-mercaptopropionic acid on Au(111), as observed by *in situ* STM imaging.[58] This short carboxylic-terminated thiol self-assembles into commensurate $p \times \sqrt{3}$ structures with $p = 5$, 7, 8, 10. An incommensurate $p \times \sqrt{3}$ lattice has also been observed. Also in this case, the difference in contrast in the STM images was assigned to molecules placed in different adsorption sites. Therefore, it is clear that family of the $p \times \sqrt{3}$ consists of upright molecules with a surface coverage very close to the $\sqrt{3} \times \sqrt{3}$ R30° lattice. This type of lattices differs completely from the striped phases consisting of lying down molecules observed for non-saturated coverage.

Rectangular (2 × $\sqrt{3}$) and (4 × $\sqrt{3}$) lattices (0.6 × 0.5 nm and 1.2 × 0.5 nm, respectively), and a molecular tilt of 50° have been recently observed by AFM for alkanethiols on the Au(111) face at non-saturated coverage.[59] However, the molecular arrangement was not discerned from the images, as contact mode AFM provides lattice resolution but not true molecular resolution. We have resolved the molecular arrangement in these lattices for propanethiolate and for annealed (T = 60 °C) hexanethiolate SAMs by high resolution STM images, as shown in Fig. 8a, c and d, respectively. Following STM data it can be concluded that the (4 × $\sqrt{3}$) involves two different sites, as proposed in ref. 59. Possible schemes for these lattices are shown in Fig. 8b and e although, as mentioned for the other lattices, the actual Au sites involved are not known. This rectangular lattices evolve towards the $\sqrt{3} \times \sqrt{3}$ R30° lattice at higher surface coverages or adsorption times.

Other type of striped phases are the so-called "pinstripe" lattices which have been observed especially for short alkanethiolates on Au(111).[60,61] These phases consist of a $\sqrt{3} \times \sqrt{3}$ R30° lattice, *i.e.* they involve standing up molecules, with periodically missing rows, as shown in Fig. 9 for a propanethiolate SAMs. The presence of missing rows in the $\sqrt{3} \times \sqrt{3}$ R30° lattice is not surprising, considering that van der Waals interactions are relatively weak for SAMs of these thiols.

The formation of ordered phases of dimethyl disulfide on the Au($\sqrt{}$111) surface has been investigated by means of LEED, XPS and DFT.[62] The LEED diffraction pattern following post-deposition annealing shows (3 × 4) domains coexisting

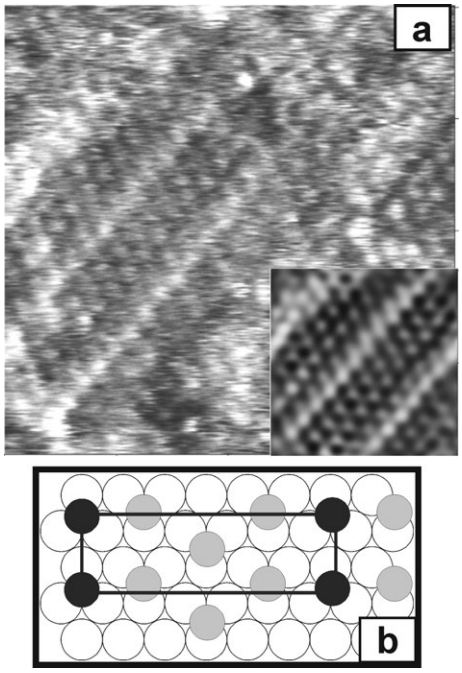

Fig. 7 (a) 10 × 10 nm^2 STM image of a 6 × $\sqrt{3}$ butanethiolate domain growing into a disordered region on Au(111). The inset shows a smaller part (5 × 5 nm^2) of the same image that has been filtered to observe more clearly the presence of butanethiolate molecules forming a $\sqrt{3} \times \sqrt{3}$ R30° lattice between the bright stripes. $E_{bias} = -965$ mV, $i_t = 205$ pA. (b) Scheme of the lattice. Black and gray circles: alkanethiolate molecules, white circles: gold atoms. The unit cell is indicated.

with the $\sqrt{3} \times \sqrt{3}$ R30° structure. XPS measurements have shown that the coverage of the (3 × 4) superstructure is the same as that of the $\sqrt{3} \times \sqrt{3}$ R30° phase. In both phases the binding energy of the S $2p_{3/2}$ core-level peak is found to be 162.2 eV, corresponding to the formation of a thiolate layer.[63] DFT calculations allowed them to identify a viable metastable (3 × 4) structure where the S headgroups of the CH_3S radicals "choose" distinct adsorption sites: 3/4 of them adsorb at bridge sites and the remaining 1/4 at on-top sites. The relative energetics of the (3 × 4) and $\sqrt{3} \times \sqrt{3}$ R30° configurations suggest that the two structures may coexist on the surface, in agreement with experimental data.

Alkanethiols which have terminal groups other than $-CH_3$ often arrange in not so common lattices. For instance, SAMs of 3-mercaptopropionic acid (MPA) on Au(111) exhibits a 3 × 3 structure coexisting with $2\sqrt{3} \times 2\sqrt{3}$ R30° and $p \times \sqrt{3}$ domains.[64] While we have shown some examples of lattices different from the $\sqrt{3} \times \sqrt{3}$ R30° and the c(4 × 2) lattices, it must be said that many others have been reported. The idea that should be kept in mind is that there is indeed a wide variety of alkanethiolate surface structures on Au(111).

2.6. Interpretation of STM images for alkanethiolate SAMs on Au(111)

An important issue that needs further investigation is the interpretation of the STM images of alkanethiolate SAMs. Despite the fact that there is no doubt that these images provide valuable information on the local surface structure at the molecular level, it is still not clear whether the STM tip "sees" the terminal group of the hydrocarbon chain, methylene units adjacent to the terminal group, or the S heads of the thiol molecules.[35,40] Some theoretical calculations made for STM imaging at high tunnelling resistance (low i_{tunnel}, high V_{bias}) favour the hypothesis that the tip actually "sees" the hydrocarbon chain or the terminal group.[40,65] However, due to the wide variety of i_{tunnel} and V_{bias} conditions used, a generalization can be oversimplifying. The reader can find a detailed

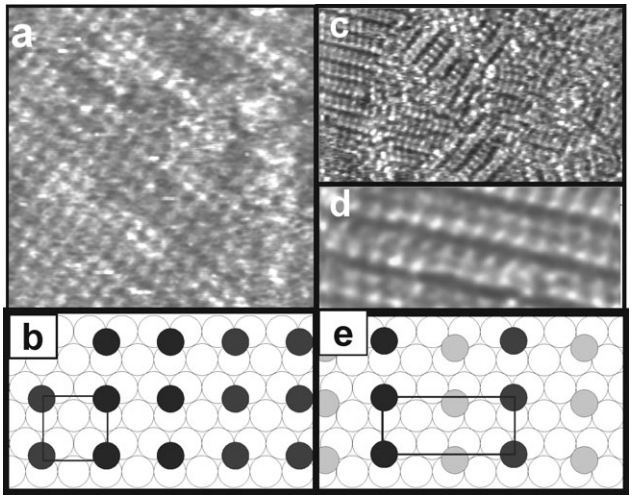

Fig. 8 (a) 6.4 × 6.4 nm^2 STM image showing a rectangular (2 × $\sqrt{3}$) propanethiolate lattice. E_{bias} = 713 mV, i_t = 2 nA. (b) Scheme showing a possible model for the (2 × $\sqrt{3}$) lattice. (c) 21.4 × 21.4 nm^2 STM image showing a rectangular (4 × $\sqrt{3}$) hexanethiolate lattice (center and left-hand side). E_{bias} = 542 mV, i_t = 500 pA. (d) STM image showing at a high resolution the (4 × $\sqrt{3}$) lattice shown in (c). (e) Scheme of the (4 × $\sqrt{3}$) lattice. (b,e) black and gray circles: alkanethiolate molecules, white circles: gold atoms. The unit cells are indicated.

discussion about the dependence of the STM images on tunneling conditions for alkanethiolate SAMs on Au in ref. 40. This interesting (and complex problem) is far from the scope of this review. Note, however, that all the surface structures discussed in this work have been observed irrespective of the STM imaging conditions (i_{tunnel}, V_{bias}) and environments (UHV, air, electrolyte solutions), and in most cases confirmed other independent techniques (AFM, LEED, GIXD, LEAD, *etc.*).

2.7. SAM defects

Among the typical defects that SAMs of alkanethiolates can present on Au(111) are (i) missing rows, especially found for short alkanethiols (Fig. 10a); (ii) vacancy Au islands produced during the self-assembly process (Fig. 10b): (iii) molecular defects, where the alkanethiolate molecules are absent or disordered (Fig. 10c), and (iv) domains boundaries, where the molecules exhibit strong disorder (Fig. 11).

Two types of missing rows have been observed: straight and zig-zag.[66] The cross section in Fig. 10a shows more clearly the alternate presence of missing rows in a 7.5 × $\sqrt{3}$ propanethiolate lattice on Au(111). The scheme indicates a possible surface arrangement for this lattice, where we have assumed alkanethiolate adsorption on hollow sites. Surface structures with missing rows can also be found as a result of some SAM annealing procedures (see below).

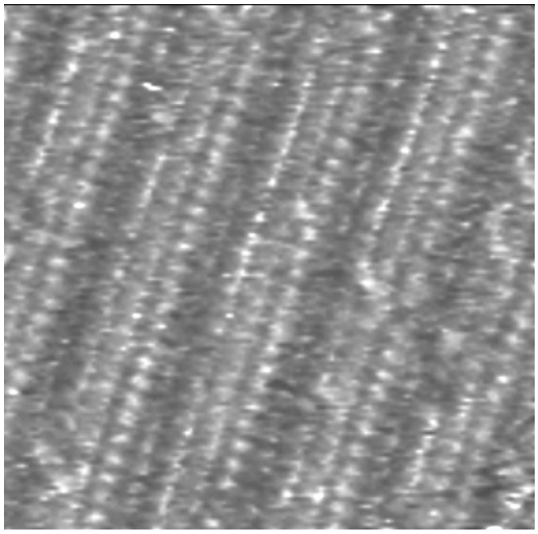

Fig. 9 11.1 × 11.1 nm^2 STM image showing a pinstripe (7.5 × $\sqrt{3}$) propanethiolate domain on Au(111). E_{bias} = 600 mV, i_t = 1 nA.

Molecular defects are present even in well-ordered, crystalline alkanethiolate domains. These SAM defects can be either molecular vacancies (also called pinholes), or regions where the molecules are not well organized, *i.e.* regions where hydrocarbon chains are not fully extended, or have a different tilt (α). The cross–section and scheme in Fig. 10c help to understand the origin of these defects at SAMs.

The commensurate molecular overlayer can adopt a number of symmetry-equivalent registries with respect to the Au lattice. Under growth conditions where the distance between nucleation events is less than the terrace size, various domains nucleate, grow, and coalesce with formation of a network of domain boundaries. The boundary between two adjacent ordered domains is a defective region in a SAM, as shown in detail in Fig. 11. Either if there are adjacent domains of different lattices (*e.g.* $\sqrt{3}$ × $\sqrt{3}$ R30° and c(4 × 2)), or two domains of the same ordered lattice with a different χ, the domain boundary consists of mismatching (or simply missing) molecules. Domain boundaries can be classified as translational, rotational or tilt boundaries.

On the other hand, the large black regions in Fig. 10b are not real SAM defects. For SAMs formed both from gas-phase and from solution it has been seen by STM and AFM, that, in addition to well-ordered domains of the above mentioned lattices, there are gold 2D vacancy islands of monatomic (0.24 nm) or diatomic (0.48 nm) depth whose bottoms are covered by the alkanethiolate molecules (Fig. 10b, cross section and scheme).[19,31,67,68] The origin of these pits could be the dissolution of gold atoms due to a weakening of the Au–Au bonds caused by the presence of the adsorbed alkanethiolate. In fact, gold has been detected in the incubation solutions, though its amount was not enough to explain the pits. Since these features are also formed for gas-phase alkanethiolate SAMs, it has been proposed that they could be caused by a substrate reconstruction. In any case, it has been reported that the pit density increases with the increasing alkanethiol concentration, and decreases with increasing length of the hydrocarbon chain. The gold substrates, in addition to vacancy islands, have other structural defects, like steps and, in the case of polycrystalline Au films, intergrain boundaries, that of course produce defects in the SAMs.

As mentioned before, defect density at SAMs depends markedly on the adsorption time, hydrocarbon chain length, the nature of the terminal groups, temperature and the substrate quality, among others. In general, defect density decreases with increasing hydrocarbon chain length. The introduction of terminal groups (S, COOH, OH, NH_2) different from the CH_3 group usually results in a decrease in the order of the monolayer.[69] Similar results have been observed by introducing benzene rings in the hydrocarbon chains.[70]

Several things can be tried to improve the quality of the films. A careful choice of solvents can yield SAMs with lower defect density.[18] Formation of SAMs at controlled potentials,[71] and repeated immersions followed by voltammetric cycles[18] have also been suggested. Adsorption from solution at T = 50–70 °C,[35,47,72,73] or soft annealing of the SAMs (T = 50–100 °C) formed at room temperature, either in air or in UHV,[19,67,74] have been proposed as means to reduce the number of defects and to obtain larger ordered domains. However, SAMs formed at controlled potentials have the same quality as those formed by simple immersion.[75,76] It is true that SAMs annealing in air or UHV lowers the number of defects, but it also produces missing rows. Annealing in solution and repetitive voltammetry and immersion seem to improve the

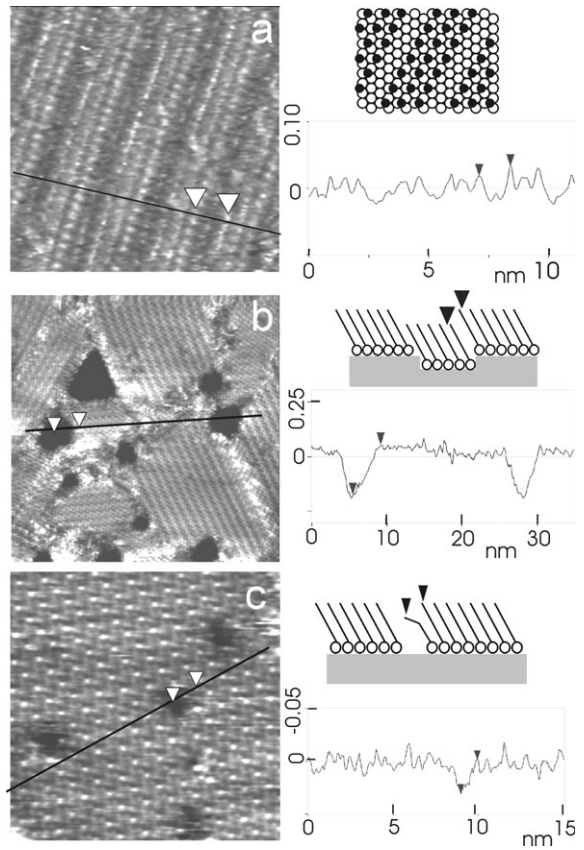

Fig. 10 Typical defects at SAMs. (a) 11.1×11.1 nm^2 STM image. Missing rows of propanethiolate molecules on Au(111). The cross-section and a scheme of a possible molecular arrangement for this lattice are shown. $E_{bias} = 600$ mV, $i_t = 1$ nm. (b) *In situ* 35 × 35 nm^2 STM image. Vacancy Au islands (black regions) in hexanethiolate-Au(111) c(4 × 2) lattices. The cross-section and a scheme of this type of defects are shown. $E_{bias} = 200$ mV, $i_t = 540$ pA. (c) *In situ* 12.6 × 12.6 nm^2 STM image. $E_{bias} = 303$ mV, $i_t = 3$ nA. Molecular defects at a c(4 × 2) hexanethiolate lattice on Au(111). The cross section and a possible scheme for these defects are depicted. b–c: Electrolyte: 0.1 M NaOH; applied potential $E = -0.7$ V *vs.* the saturated calomel electrode (SCE).

layers, but actually none of these procedures really yields a defect-less monolayer.

As an example of the combined effects of temperature and chain length we can mention a study of the thermal stability of short alkanethiol ($n < 9$) and long ($n = 18$) SAMs.[77] Results from grazing angle reflection-absorption IR, cyclic voltammetry, and molecular dynamics simulation show that short-chain alkanethiols ($n < 8$) are more defective at lower temperature than long-chain alkanethiols. With increasing temperature, disorder in the SAM tends to increase, but for short-chain SAMs it saturates at temperatures below 360 K, so that any further increase in temperature does not lead to any significant change in conformational order, until desorption occurs. In contrast, the disorder in the long-chain SAM increases monotonically with temperature beyond 360 K.[77]

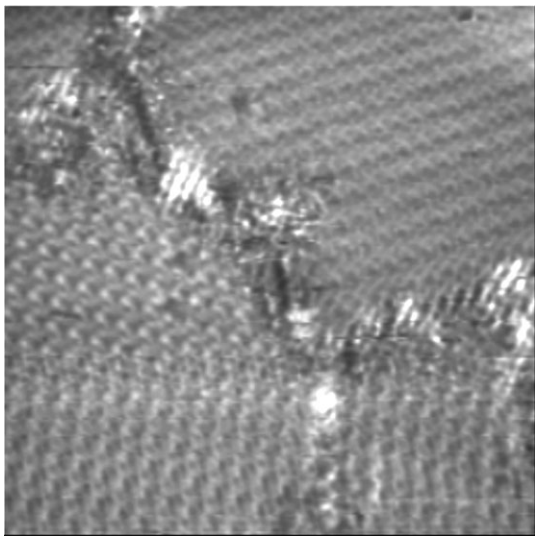

Fig. 11 20 × 20 nm^2 STM image showing domains boundaries between rotated c(4 × 2) domains. $E_{bias} = 200$ mV, $i_t = 740$ pA.

For many SAM applications the quality of SAMs prepared in "standard" conditions is enough, but for others defects are a problem and the control of SAMs quality is a crucial point. A typical example where high-quality SAMs are required is in the field of electronics and spintronics. Although alkanethiolate SAMs are certainly not the best candidates for these applications (due to their high mobility and low conductance), similar defects as those shown in Fig. 10 should be present also in more "promising" phenyl-and non-saturated thiols.[78] In the case of molecular electronics and spintronics, metallization of the thiol SAMs is often needed to build different types of devices. However, during metallization from the gas phase, SAM defects enable the diffusion of metal adatoms, thus connecting the deposited metal layer with the substrate, and leading to inefficient systems. Degradation of the SAMs quality during thermal vapour deposition has also been observed, in agreement with the above mentioned experimental and theoretical results. The "top contact problem" is one of the biggest problems with molecule-based devices, and results in poor yields. Often, the overall device yield will be significantly less than 10%, and sometimes less than 1%. The substrate quality also plays an important role in the SAMs stability: it has been reported that substrate-induced linear defects dramatically increase the oxidation rate of the alkanethiolate molecules (to form sulfonates), even in the darkness.[79] The oxidized products desorb from the surface and decompose under X-ray irradiation in UHV. Therefore, great efforts have been done to improve SAMs quality by decreasing defect size and density (as mentioned before), or to decrease metal diffusion by the presence of specific terminal groups.

From a positive point of view, defects at SAMs can be used to build nanocontacts and to prepare small metallic nanoclusters by confined growth at defects. From the basic point of view, defects are important for the understanding of charge transfer through SAMs. In fact, most of the present studies are focused on tunnelling mechanisms through the hydrocarbon chain. If, however, defects are present, they offer an alternative path for charge transfer. In fact, electrochemical measurements of Au(111) substrates modified by alkanethiols of different chain length and/or terminal group in methylene blue (MB) solutions have revealed that the MB redox couple is reversible, independent of the alkanethiol chain length (or the terminal group). This evidence, and the fact that the charge transfer was hindered when diminishing the defect density (by gentle annealing in solution), lead to the conclusion that, at least in that case, electron transfer occurred mainly through defects, and not through a tunnelling mechanism.[61,80]

2.8. Mixed SAMs

Multi-component (or mixed) thiol SAMs are interesting systems to control the surface energy, and thus the wetting properties, of the monolayers by "tuning" the surface concentration of the different components.[3,13a,19,35,73] The idea of patterning SAMs with two or more thiols is very attractive for many applications. It could provide a way to use a bottom-up technologies to obtain patterns that nowadays can in general only be achieved with lithographical techniques. But even without forming ordered structures at the nano or micrometer scale, mixed SAMs are important because it has been found that some species (like biomolecules) can be better

anchored on these SAMs,[81] and also that electron transfer of immobilized species is sometimes more efficient if the electroactive thiol is "diluted" with a non-electroactive thiol.[18,81]

There are two methods to prepare mixed thiol SAMs: coadsorption from solutions containing thiol mixtures and adsorption of asymmetric disulfides.[3] It must be said that the mole fraction in the SAM is not the same as that in the immersion solution, especially when the chain lengths are very different. The first method is more versatile, since with disulfides it is more difficult to obtain mixed SAMs with mole fractions very different from 0.5.

Several studies have been performed with different thiol mixtures and under different conditions, and there has been some controversy about the possibility of obtaining separated domains by playing with the solvent, the nature of the thiols or the temperature.[3,73] Phase segregation can be sometimes achieved when the components have very different chain lengths and/or different functionalities (either terminal or internal),[73] but the truth is that the domains in general are quite small. Also, mixed monolayers tend to be more defective than the corresponding single-component SAMs.

2.9. Dynamics

The dynamics of ordered domains of adsorbed atoms and molecules on solid substrates, and the structural transformations that take place in these domains has been of interest in the last past years. To study this kind of processes, high quality real time imaging at the atomic or molecular level is required. STM and AFM fulfil these requirements, but, in any case, relatively few atomic-or molecular-level dynamical studies have been performed. In particular, in the case of alkanethiolates on Au(111), in spite of the great number of studies that these systems have inspired, relatively little is known about their dynamics for well-ordered SAMs.

In some STM and AFM studies in air, real-time transformations from the $\sqrt{3} \times \sqrt{3}$ R30° lattice to the c(4 × 2) lattice had been reported, and thus for some time it was believed that the latter was the most stable structure on Au(111).[82] Terán Arce *et al.*[83] reported on the structural dynamics of alkanethiol monolayers on Au(111), and presented images taken in air and in pure alkanethiol which show the evolution of the surface structures. Their results showed an initial gas-like adsorption stage, where monatomic deep pit clustering occurs, followed by an advanced adsorption stage in which adlayer structure changes from $p \times \sqrt{3}$ (standing-up molecules) to $\sqrt{3} \times \sqrt{3}$ R30°, that in turn fluctuates with the c(4 × 2) lattice. The first stage was interpreted as the movement of thiols from fcc to hcp sites, and the second was explained by fluctuations of molecules from hollow to bridge sites. Structural fluctuations at adsorbate domains occurred simultaneously with fluctuations in the size of monatomic pits. All these measurements were performed at 298 K. The fact that real time imaging showed reversible $\sqrt{3} \times \sqrt{3}$ R30° ⇔ c(4 × 2) transformations strongly suggested that both lattices had nearly the same energy. It was then thought that, since the transformations between different surface structures should involve some kind of rearrangement or displacement of the molecules, the process would be hindered in aqueous media (where hydrophobic forces tend to stabilize the adsorbed layer even more).

However, recent *in situ* STM results of hexanethiolate SAMs have revealed the existence of the same reversible $\sqrt{3} \times \sqrt{3}$ R30° ⇔ c(4 × 2) transitions also in aqueous (NaOH 0.1 M) solutions[84] (Fig. 12). These transitions are independent of the applied potential (E) in the $-0.8\ V < E < -0.4\ V$ range. Although it seems that time or annealing favour the formation of the c(4 × 2) lattice, recent DFT calculations indicate that the energy difference between the $\sqrt{3} \times \sqrt{3}$ R30° and c(4 × 2) structures is very small.[41c,d] The *in situ* STM results support the idea that the two surface structures have almost the same

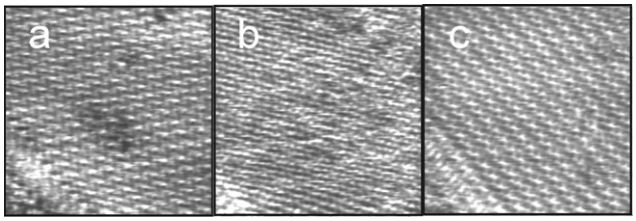

Fig. 12 13.3 × 13.3 nm^2 *in situ* STM images of hexanethiolate SAM on Au(111) taken in 0.1 M NaOH aqueous solution. (a) Rectangular c(4 × 2). E_{bias} = 200 mV, i_t = 794 pA, (b) $\sqrt{3} \times \sqrt{3}$ R30°. E_{bias} = 200 mV, i_t = 794 pA, (c) Zig-zag c(4 × 2). E_{bias} = 200 mV, i_t = 794 pA. These transitions take place in a few minutes.

energy. The interaction of the STM tip with the alkanethiolate SAM would also provide the necessary energy to go from one structure to the other. Repair and formation of molecular defects were also imaged for this system.[84]

Potential induced transformations in electrolyte solutions have been also reported.[84,85] These transformations involve two steps: electrodesorption of chemisorbed alkanethiol molecules from Au(111) terraces, producing physisorbed nanometer-sized aggregates of alkanethiolates, and final electrodesorption of alkanethiol molecules that remained chemisorbed at step edges due to the increased coordination number at these substrate sites.[86]

3. Conclusions and outlook

The surface structures of alkanethiolate lattices on Au(111) have been reviewed, showing the richness of what is often considered as a simple surface science model system. A key point that deserves further investigation is the determination of the adsorption sites for the different surfaces structures. In this field, kinetics and thermodynamics should be incorporated to understand the structure and evolution of alkanethiolate SAMs. The presence of local minima in nanostructures and their dynamics is an interesting field that should be explored. Different defects have been shown and discussed. These defects could be interesting to develop nanocontacts and to growth nanoparticles in confined environments. On the other hand, the control of defects in alkanethiolates, which are relatively simple systems, should help us to eliminate or at least reduce defects in SAMs of other less studied thiols that are promising in the field of molecular electronics and spintronics, and also to build effective organic barriers for corrosion protection. In this context, new routes to produce dense and defect-free SAMs will be needed in a near future.

List of acronyms

AES: Auger electron spectroscopy
AFM: Atomic force microscopy
DFT: Density functional theory
fcc: Face centered cubic
GIXD: Grazing Incidence X-ray diffraction
hcp: Hexagonal closed packed
HOPG: Highly ordered Pirolytic graphite
IR: Infra Red
LEAD: Low energy atom diffraction
LEED: Low energy electron diffraction
SAM: Self assembled monolayer
SFG: Sum frequency generation
STM: Scanning tunneling microscopy
TPD: Temperature programmed desorption
UHV: Ultra high vacuum
XPD: X-ray photoelectron diffraction
XPS: X-ray photoelectron spectroscopy
XRD: X-ray diffraction
XSW: X-ray standing wavefield absorption

Acknowledgements

This work was supported by the Agencia Nacional de Promoción Científica y Tecnológica (PICT 02-11111). M.E.V. is a member of the research career of CIC. Authors thank G. Andreasen and F. Terán Arce for taking some of the STM images shown.

References

1 J. L. Wilbur and G. M. Whitesides, in *Nanotechnology*, ed. G. Timp, Springer Verlag, New York, 1999, ch. 8.
2 J. C. Love, L. A. Estroff, J. K. Kriebel, R. G. Nuzzo and G. M. Whitesides, *Chem. Rev.*, 2005, **105**, 1103.
3 B. D. Gates, Q. Xu, M. Stewart, D. Ryan, C. G. Willson and G. M. Whitesides, *Chem. Rev.*, 2005, **105**, 1171.
4 W. C. Bigelow, D. L. Pickett and W. A. Zisman, *J. Colloid Interface Sci.*, 1946, **1**, 513.
5 (*a*) A. Ulman, *An Introduction to Ultrathin Organic Films: from Langmuir-Blodgett to Self-assembly*, Academic Press, San Diego, CA, 1991; (*b*) A. Ulman, *Chem. Rev.*, 1996, **96**, 1533.
6 L. H. Dubois and R. G. Nuzzo, *Annu. Rev. Phys. Chem.*, 1992, **43**, 437.
7 J. N. Israelachvili, *Intermolecular and Surface Forces*, Academic Press, London, 1994.
8 (*a*) R. H. Terrill, T. A. Postlethwaite, C. H. Chen, C. D. Poon, A. Terzis, A. Chen, J. E. Hutchison, M. R. Clark, G. D. Wignall, J. D. Londono, R. Superfine, M. Falvo, C. S. Johnson, E. T. Samulski and R. W. Murray, *J. Am. Chem. Soc.*, 1995, **117**, 12537; (*b*) B. R. Martin, D. J. Dermody, B. D. Reiss, M. M. Fang, L. A. Lyon, M. J. Natan and T. E. Mallouk, *Adv. Mater.*, 1999, **11**, 1021.
9 (*a*) O. Azzaroni, P. L. Schilardi and R. C. Salvarezza, in *Encyclopedia of Nanoscience and Nanotechnology*, ed. H. S. Nalwa, American Scientific Publishers, Stevenson Ranch, CA, 2004, **vol. 5**, p. 835; (*b*) O. Azzaroni, M. Fonticelli, G. Benítez, P. L. Schilardi, R. Gago, I. Caretti, L. Vázquez and R. C. Salvarezza, *Adv. Mater.*, 2004, **16**, 405.
10 J. Sagiv, *J. Am. Chem. Soc.*, 1980, **102**, 92.
11 R. G. Nuzzo and D. L. Allara, *J. Am. Chem. Soc.*, 1983, **105**, 4481.
12 D. L. Allara and R. G. Nuzzo, *Langmuir*, 1985, **1**, 45.
13 (*a*) F. Schreiber, *Prog. Surf. Sci.*, 2000, **65**, 151; (*b*) F. Schreiber, *J. Phys.: Condens. Matter*, 2004, **16**, R881.
14 D. G. Castner and B. D. Ratner, in *Frontiers in Surface and Interface Science*, ed. C. B. Duke and E. W. Plummer, North Holland, Amsterdam, 2002.
15 See for instance, *Scientific American*, vol. 285 Issue 3 (Sept 2001), *Science: Supramolecular Chemistry and Self Assembly*, vol. 295, pp. 2313–2556 (2002).
16 M.-C. Daniel and D. Astruc, *Chem. Rev.*, 2004, **104**, 293.
17 U. Drechsler, B. Erdogan and V. M. Rotello, *Chem. – Eur. J.*, 2004, **10**, 5570.
18 (*a*) H. O. Finklea, in *Electroanalytical Chemistry*, ed. A. J. Bard, I. Rubinstein, Marcel Dekker, New York, 1996, Vol 19, p. 109; (*b*) H. O. Finklea, in *Encyclopedia of Analytical Chemistry: Applications, Theory and Instrumentation*, ed. R. A. Meyers, Wiley & Sons, New York, 2000.
19 G. E. Poirier, *Chem. Rev.*, 1997, **97**, 1117.
20 D. K. Schwartz, *Annu. Rev. Phys. Chem.*, 2001, **52**, 107.
21 D. P. Woodruff and T. A. Delchar, *Modern Techniques of Surface Science*, Cambridge University Press, Cambridge, 2nd edn, 1994.
22 (*a*) G. Binnig, H. Rohrer, C. Gerber and E. Weibel, *Appl. Phys. Lett.*, 1982, **40**, 178; (*b*) G. Binnig and H. Rohrer, *Helv. Phys. Acta*, 1982, **55**, 726; (*c*) G. Binnig, H. Rohrer, C. Gerber and E. Weibel, *Phys. Rev. Lett.*, 1982, **49**, 57.
23 *Scanning Tunneling Microscopy I*, ed. H.-J. Güntherodt and R. Wiesendanger, Springer-Verlag, Berlin, 1994.
24 *Scanning Tunneling Microscopy and Related Methods*, ed. R. J. Behm, N. García and, H. Rohrer, NATO ASI Series, Kluwer, Dordrecht, 1990.
25 S. N. Magonov and M.-H. Whangbo, *Surface Analysis with STM and AFM*, VCH, Weinheim, 1996.
26 *Scanning Tunneling Microscopy and Spectroscopy*, ed. D. A. Bonnell, VCH, Weinheim, 1993.
27 A. M. Rampi, R. E. Holmlin and G. M. Whitesides, *J. Am. Chem. Soc.*, 1999, **121**, 7895.
28 A. Lio, D. H. Charych and M. Salmeron, *J. Phys. Chem. B*, 1997, **101**, 3800.
29 Y.-J. Han and J. Aizenberg, *Angew. Chem., Int. Ed.*, 2003, **42**, 3668.
30 F. Schreiber, A. Eberhardt, T. Y. B. Leung, P. Schwartz, S. M. Wetterer, D. J. Lavrich, L. Berman, P. Fenter, P. Eisenberger and G. Scoles, *Phys. Rev. B: Condens. Matter*, 1998, **57**, 12476.
31 S. Xu, S. J. N. Cruchon-Dupeyrat, J. C. Garno, G.-Y. Liu, G. K. Jennings, T.-H. Yong and P. E. Laibinis, *J. Chem. Phys.*, 1998, **108**, 5002.
32 G. E. Poirier and E. D. Pylant, *Science*, 1996, **272**, 1145.
33 R. Yamada and K. Uosaki, *Langmuir*, 1998, **14**, 855.
34 F. Terán Arce, M. E. Vela, R. C. Salvarezza and A. J. Arvia, *Surf. Rev. Lett.*, 1997, **4**, 637.
35 E. Delamarche, B. Michel, H. A. Biebuyck and C. Gerber, *Adv. Mater.*, 1996, **8**, 719.
36 (*a*) L. Strong and G. M. Whitesides, *Langmuir*, 1988, **4**, 546; (*b*) C. E. D. Chidsey and D. N. Loiacono, *Langmuir*, 1990, **6**, 682; (*c*) C. E. D. Chidsey, G.-Y. Liu, P. Rowntree and G. Scoles, *J. Chem. Phys.*, 1989, **91**, 4421; (*d*) L. H. Dubois, B. R. Zegarski and R. G. Nuzzo, *J. Chem. Phys.*, 1993, **98**, 678; (*e*) M. G. Samant, C. A. Brown and J. G. Gordon II, *Langmuir*, 1991, **7**, 437; (*f*) C. A. Widrig, C. A. Alves and M. D. Porter, *J. Am. Chem. Soc.*, 1991, **113**, 2807.
37 P. Fenter, P. Eisenberger and K. S. Liang, *Phys. Rev. Lett.*, 1993, **70**, 2447.
38 N. Camillone III, C. E. D. Chidsey, G.-Y. Liu and G. Scoles, *J. Chem. Phys.*, 1993, **98**, 3503.
39 H. Basch and M. A. Ratner, *J. Chem. Phys.*, 2003, **119**, 11926.
40 (*a*) C. Zeng, B. Li, B. Wang, H. Wang, K. Wang, J. Yang, J. G. Hou and Q. Zhu, *J. Chem. Phys.*, 2002, **117**, 851; (*b*) B. Li, C. Zeng, Q. Li, B. Wang, L. Yuan, H. Wang, J. Yang, J. G. Hou and Q. Zhu, *J. Phys. Chem. B*, 2003, **107**, 972.
41 (*a*) K. M. Beardmore, J. D. Kress, A. R. Bishop and N. Grønbech-Jensen, *Synth. Met.*, 1997, **84**, 317; (*b*) K. M. Beardmore, J. D. Kress, N. Grønbech-Jensen and A. R. Bishop, *Chem. Phys. Lett.*, 1998, **286**, 40; (*c*) H. Grönbeck, A. Curioni and W. Andreoni, *J. Am. Chem. Soc.*, 2000, **122**, 3839; (*d*) Y. Yourdshahyan, H. K. Zhang and A. M. Rappe, *Phys. Rev. B: Condens. Matter*, 2001, **63**, 81405R; (*e*) M. C. Vargas, P. Gianozzi, A. Selloni and G. Scoles, *J. Phys. Chem. B*, 2001, **105**, 9509; (*f*) T. Hayashi, Y. Morikawa and H. Nozoye, *J. Chem. Phys.*, 2001, **114**, 7615; (*g*) Y. Akinaga, T. Nakajima and K. Hirao, *J. Chem. Phys.*, 2001, **114**, 8555; (*h*) J. Gottschalck and B. Hammer, *J. Chem. Phys.*, 2002, **116**, 784; (*i*) Y. Yourdshahyan and A. Rappe, *J. Chem. Phys.*, 2002, **117**, 825.
42 H. Kondoh, M. Iwasaki, T. Shimada, K. Amemiya, T. Yokohama, T. Ohta, M. Shimomura and S. Kono, *Phys. Rev. Lett.*, 2003, **90**, 66102.
43 M. G. Roper, M. P. Skegg, C. J. Fisher, J. J. Lee, V. R. Dhanak, D. P. Woodruff and R. G. Jones, *Chem. Phys. Lett.*, 2004, **389**, 87.
44 X. Torrelles, C. Vericat, M. E. Vela, M. H. Fonticelli, M. A. Daza Millone, R. Felici, T.-L. Lee, J. Zegenhagen, G. Muñoz, J. A. Martín-Gago and R. C. Salvarezza, submitted.
45 R. G. Nuzzo, E. M. Korenic and L. H. Dubois, *J. Chem. Phys.*, 1990, **93**, 767.
46 G. E. Poirier and M. J. Tarlov, *Langmuir*, 1994, **10**, 2853.
47 E. Delamarche, B. Michel, C. Gerber, D. Anselmetti, H.-J. Güntherodt, H. Wolf and H. Ringsdorf, *Langmuir*, 1994, **10**, 2869.
48 D. Anselmetti, A. Baratoff, H.-J. Güntherodt, E. Delamarche, B. Michel, C. Gerber, H. Kang, H. Wolf and H. Ringsdorf, *Europhys. Lett.*, 1994, **27**, 365.
49 M. S. Yeganeh, S. M. Dougal, R. S. Polizzotti and P. Rabinowitz, *Phys. Rev. Lett.*, 1995, **74**, 1811.
50 P. Fenter, A. Eberhardt and P. Eisenberger, *Science*, 1994, **266**, 1216.
51 P. Fenter, F. Schreiber, L. Berman, G. Scoles, P. Eisenberger and M. J. Bedzyk, *Surf. Sci.*, 1998, **412/413**, 213.
52 F. Terán Arce, M. E. Vela, R. C. Salvarezza and A. J. Arvia, *J. Chem. Phys.*, 1998, **109**, 5703.
53 X. Torrelles, E. Barrena, C. Munuera, J. Rius, S. Ferrer and C. Ocal, *Langmuir*, 2004, **20**, 9396.
54 G. E. Poirier, W. P. Fitts and J. M. White, *Langmuir*, 2001, **17**, 1176.
55 S.-B. Darling, A. W. Rosembaum, Y. Wang and S. J. Siberner, *Langmuir*, 2002, **18**, 7462.
56 J. Noh and M. Hara, *RIKEN Rev.*, 2001, **38**, 49.
57 K. Kobayashi, H. Yamada, T. Horiuchi and K. Matsushige, *Jpn. J. Appl. Phys., Part. 1*, 1998, **37**, 6183.
58 M. J. Giz, B. Duong and N. J. Tao, *J. Electroanal. Chem.*, 1999, **465**, 92.

59 E. Barrena, E. Palacios-Lidón, C. Munuera, X. Torrelles, S. Ferrer, U. Jonas, M. Salmeron and C. Ocal, *J. Am. Chem. Soc.*, 2004, **126**, 385.
60 H. Hagenstrom, M. E. Schneeweiss and D. M. Kolb, *Langmuir*, 1998, **15**, 2435.
61 G. Benítez, C. Vericat, S. Tanco, F. Remes Lenicov, M. F. Castez, M. E. Vela and R. C. Salvarezza, *Langmuir*, 2004, **20**, 5030.
62 V. De Renzi, D. Marchetto, R. Biagi, U. del Pennino, R. Di Felice and A. Selloni, *J. Phys. Chem. B*, 2004, **108**, 16.
63 C. Vericat, M. E. Vela, G. Andreasen, R. C. Salvarezza, L. Vázquez and J. A. Martín-Gago, *Langmuir*, 2001, **17**, 4919.
64 T. Sawaguchi, Y. Sato and F. Mizutani, *Phys. Chem. Chem. Phys.*, 2001, **3**, 3399.
65 P. Paredes Olivera and M. Patrito, presented at FyQS I Meeting, Bariloche, Argentina, 2004, http://cabcat1.cnea.gov.ar/~colato/grupos/superficies/fyqs/FyQSI_abstractbook.doc.
66 C. Schönenberger, J. Jorritsma, J. A. M. Sondag-Huethorst and L. G. J. Fokkink, *J. Phys. Chem.*, 1995, **99**, 3259.
67 J.-P. Bucher, L. Santesson and K. Kern, *Langmuir*, 1994, **10**, 979.
68 J. A. M. Sondag-Huethorst, C. Schönenberger and L. G. J. Fokkink, *J. Phys. Chem.*, 1994, **98**, 6826.
69 O. Azzaroni, M. E. Vela, H. Martín, A. Hernández Creus, G. Andreasen and R. C. Salvarezza, *Langmuir*, 2001, **17**, 6647.
70 C. H. Kagan, presented at NFS-CONICET Quilmes Nanoscience Workshop: Electronics with Molecules and Quantum Dots, 2003.
71 C. M. A. Brett, S. Kresak, T. Hianik and A. M. Oliveira Brett, *Electroanalysis*, 2003, **15**, 557.
72 L. A. Bumm, J. J. Arnold, L. F. Charles, T. D. Dunbar, D. L. Allara and P. S. Weiss, *J. Am. Chem. Soc.*, 1999, **121**, 8017.
73 P. A. Lewis, Z. J. Donhauser, B. A. Mantooth, R. K. Smith, L. A. Bumm, K. F. Kelly and P. S. Weiss, *Nanotechnology*, 2001, **12**, 231.
74 O. Cavalleri, A. Hirstein, J.-P. Bucher and K. Kern, *Thin Solid Films*, 1996, **284–285**, 392.
75 D. E. Weisshaar, B. D. Lamp and M. D. Porter, *J. Am. Chem. Soc.*, 1992, **114**, 5860.
76 T. Sumi and K. Uosaki, *J. Phys. Chem. B*, 2004, **108**, 6422.
77 N. Prathima, M. Harini, Neeraj Rai, R. H. Chandrashekara, K. G. Ayappa, S. Sampath and S. K. Biswas, *Langmuir*, 2005, **21**, 2364.
78 (*a*) Y. Tai, A. Shaporenko, W. Eck, M. Grunze and M. Zharnikov, *Langmuir*, 2005, **20**, 7166; (*b*) Y. Tai, A. Shaporenko, H.-T. Rong, M. Buck, W. Eck, M. Grunze and M. Zharnikov, *J. Phys. Chem. B*, 2004, **108**, 16806.
79 M. T. Lee, C. Hsue, M. S. Freund and G. S. Ferguson, *Langmuir*, 1998, **14**, 6419.
80 C. Vericat, F. Remes Lenicov, S. Tanco, G. Andreasen, M. E. Vela and R. C. Salvarezza, *J. Phys. Chem. B*, 2002, **106**, 9114.
81 K. Fujita, N. Nakamura, H. Ohno, B. S. Leigh, K. Niki, H. B. Gray and J. H. Richards, *J. Am. Chem. Soc.*, 2004, **126**, 13954.
82 I. Touzov and C. B. Gorman, *J. Phys. Chem. B*, 1997, **101**, 5263.
83 F. Terán Arce, M. E. Vela, R. C. Salvarezza and A. J. Arvia, *Langmuir*, 1998, **14**, 7203.
84 C. Vericat, G. Andreasen, M. E. Vela, H. Martín and R. C. Salvarezza, *J. Chem. Phys.*, 2001, **115**, 6672.
85 D. Hobara, K. Miyake, S. I. Imabayashi, K. Niki and T. Kakiuchi, *Langmuir*, 1998, **14**, 3590.
86 H. Martin, C. Vericat, G. Andreasen, M. E. Vela and R. C. Salvarezza, *J. Chem. Phys.*, 2002, **117**, 2293.

